

# Data-driven system identification using quadratic embeddings of nonlinear dynamics

Stefan Klus<sup>1</sup> and Joel-Pascal N’Konzi<sup>2</sup>

<sup>1</sup>School of Mathematical & Computer Sciences, Heriot-Watt University, Edinburgh, UK

<sup>2</sup>Maxwell Institute for Mathematical Sciences, University of Edinburgh and Heriot-Watt University, Edinburgh, UK

## Abstract

We propose a novel data-driven method called QENDy (*Quadratic Embedding of Nonlinear Dynamics*) that not only allows us to learn quadratic representations of highly nonlinear dynamical systems, but also to identify the governing equations. The approach is based on an embedding of the system into a higher-dimensional feature space in which the dynamics become quadratic. Just like SINDy (*Sparse Identification of Nonlinear Dynamics*), our method requires trajectory data, time derivatives for the training data points, which can also be estimated using finite difference approximations, and a set of preselected basis functions, called *dictionary*. We illustrate the efficacy and accuracy of QENDy with the aid of various benchmark problems and compare its performance with SINDy and a deep learning method for identifying quadratic embeddings. Furthermore, we analyze the convergence of QENDy and SINDy in the infinite data limit, highlight their similarities and main differences, and compare the quadratic embedding with linearization techniques based on the Koopman operator.

## 1. Introduction

Over the last few years, many data-driven approaches for the analysis of complex dynamical systems have been proposed that are based on the Koopman operator or its infinitesimal generator. The Koopman operator provides a linear representation of the typically highly nonlinear dynamics, describing the system in terms of *observables* and their evolution in time [1, 2, 3]. Its eigenvalues and eigenfunctions, often estimated from trajectory data, contain important information about global properties such as inherent time scales and associated spatiotemporal patterns [4, 5, 6]. Applications include the detection of metastable sets, system identification, stability analysis, forecasting, and control [7, 8, 9, 10, 11, 12, 13], see [14] for a detailed overview and additional references. However, the linearity of the Koopman operator comes at a cost—namely, the representation is *infinite-dimensional*. The Koopman operator framework is also closely related to Carleman linearization techniques [15, 16, 17]. If we allow not only linear but also quadratic representations, it is always possible to obtain a *finite-dimensional* model as shown in [18, 19], provided that the system comprises only elementary functions such as polynomial, trigonometric, exponential, logarithmic, and rational functions (including compositions thereof). The reformulation process—sometimes called *quadratization* or in general *polynomialization*—is based on successively defining new variables and applying the chain rule. Similar ideas have also been used in [20, 21, 22, 23, 24, 25, 26, 27]. Bounds on the number of required additional variables are known, see, e.g., [19], but the quadratic embedding itself is in general not uniquely defined. A quadratic embedding of the dynamics can be regarded as a compromise between a highly nonlinear but low-dimensional model and a linear but infinite-dimensional model.

Instead of using the Koopman operator or generator for system identification and forecasting, we develop a method that is similar in spirit, but relies on a quadratic embedding instead of a Koopman or Carleman linearization. The main goal is again to reformulate nonlinear dynamical systems using a model structure that is as simple as possible but still able to capture complicated dynamical behavior and can be easily estimated from simulation or measurement data. These quadratic systems can then be combined with model reduction, optimization, model predictive control, or uncertainty quantification techniques tailored to such problems. A deep learning method for identifying quadratic embeddings was proposed in [28]. While such an approach is extremely flexible and versatile, the learned dynamical systems typically lack interpretability and often do not generalize well to unseen data. Another drawback is that the method requires solving an optimization problem involving a linear combination of three potentially contradictory loss functions so that we obtain only an *optimal compromise*, i.e., one point of the Pareto set.

Our method, which we call *Quadratic Embedding of Nonlinear Dynamics* (QENDy), on the other hand, is closely related to the *Sparse Identification of Nonlinear Dynamics* (SINDy) method [29], which directly estimates the governing equations and can be regarded as a special case of a Koopman generator estimation as shown in [12]. This allows us to not only identify the quadratic embedding, but also to extract the governing equations, which can then be written in terms of the functions contained in the dictionary. Furthermore, we show that an optimal solution of the resulting optimization problem can be obtained by solving systems of linear equations. In this sense, our method is closely related to the operator inference framework for learning reduced-order models from data by postulating a polynomial dynamical system in the reduced space [30]. An open question—regarding not only QENDy and SINDy, but also methods for approximating the Koopman operator such as *Extended Dynamic Mode Decomposition* (EDMD) and its extensions [31, 5, 6]—is the choice of suitable basis functions. Given a sufficiently large dictionary, SINDy uses sparse approximation techniques to identify parsimonious models. That is, the goal is to represent the vector field by a linear combination of only a few basis functions. QENDy, on the other hand, uses a dictionary to define a typically nonlinear mapping from the original state space to a higher-dimensional embedding space and then learns a quadratic model in this embedded space. Relationships between these different modeling approaches will be discussed in more detail below. The main contributions of this work are as follows:

- i) We first derive a method called QENDy for learning quadratic embeddings of nonlinear ordinary differential equations, given a set of training data points and a dictionary containing basis functions.
- ii) We analyze the convergence of QENDy and SINDy in the infinite data limit and show that both methods can be interpreted in terms of best approximations.
- iii) We present numerical results for benchmark problems and compare the efficacy and accuracy of QENDy, SINDy, and an autoencoder-based method for learning quadratic embeddings.

We will start with an introduction to the quadratic embedding framework and several guiding examples in Section 2 and then derive an optimization problem that allows us to identify the optimal quadratic embedding for a given feature space in Section 3. Numerical results will be presented in Section 4 and concluding remarks and open problems in Section 5.

## 2. Quadratic reformulation of nonlinear dynamical systems

Given an autonomous ordinary differential equation

$$\dot{x} = F(x), \tag{1}$$

with  $F: \mathbb{R}^n \rightarrow \mathbb{R}^n$ , we embed the state  $x$  into an  $N$ -dimensional feature space via

$$z := \phi(x) = \begin{bmatrix} \phi_1(x) \\ \vdots \\ \phi_N(x) \end{bmatrix},$$

where  $\phi: \mathbb{R}^n \rightarrow \mathbb{R}^N$  and  $N > n$ . We call  $\{\phi_i\}_{i=1}^N$  the *set of basis functions* or *dictionary*. Using the chain rule, we obtain

$$\dot{z} = \underbrace{\begin{bmatrix} \nabla \phi_1^\top(x) \\ \vdots \\ \nabla \phi_N^\top(x) \end{bmatrix}}_{=: J(x)} \dot{x} = J(x) F(x).$$

The idea is to lift the original dynamics to a higher-dimensional space in such a way that we obtain a quadratic ordinary differential equation of the form

$$\dot{z} = A(z \otimes z) + Bz + C, \quad (2)$$

with  $A \in \mathbb{R}^{N \times N^2}$ ,  $B \in \mathbb{R}^{N \times N}$ , and  $C \in \mathbb{R}^N$ , where  $\otimes$  denotes the Kronecker product. Any nonlinear ordinary differential equation—provided it can be written in terms of compositions of elementary functions—can be reformulated as a quadratic system in a higher-dimensional feature space, see, e.g., [18, 19].

**Remark 2.1.** Before we continue with an illustrative example, a few remarks are in order:

- i) Let  $\mathcal{L}$  denote the infinitesimal generator of the Koopman operator associated with (1), which for an observable  $f$  is defined by

$$\mathcal{L}f = F \cdot \nabla f,$$

we can also write the quadratic system as  $\dot{z} = \mathcal{L}\phi$ , where the generator is applied component-wise.

- ii) Since  $z \otimes z$  contains  $z_i z_j$  and also  $z_j z_i$ , some columns of the matrix  $A$  are clearly redundant. Reshaping each row of  $A$  as an  $N \times N$  matrix, we could simply store only the upper-triangular part or assume w.l.o.g. that the matrix is symmetric, reducing the overall number of degrees of freedom from  $N^3$  to  $\frac{N^2(N+1)}{2}$ . However, for the sake of clarity, we will work with the full matrix  $A$ .

- iii) Instead of using a matrix  $A \in \mathbb{R}^{N \times N^2}$ , we could also define a tensor  $A \in \mathbb{R}^{N \times N \times N}$ . This would allow us to use low-rank tensor approximation techniques (e.g., matrix product states [32] or, equivalently, the tensor-train format [33]) and to potentially mitigate the curse of dimensionality.

**Example 2.2.** Given the differential equation  $\dot{x} = \frac{1}{1+e^x}$ , we first define  $\dot{z}_1 = z_2$  and  $z_2 = \frac{1}{1+e^{z_1}}$ , which implies

$$\dot{z}_2 = -\frac{1}{(1+e^{z_1})^2} e^{z_1} z_1 = -z_2^3 e^{z_1}.$$

Adding  $z_3 = e^{z_1}$ , we then obtain

$$\begin{aligned} \dot{z}_1 &= z_2, \\ \dot{z}_2 &= -z_2^3 z_3, \\ \dot{z}_3 &= e^{z_1} \dot{z}_1 = z_2 z_3. \end{aligned}$$

Finally, defining  $z_4 = z_2^2 z_3$  yields

$$\begin{aligned}\dot{z}_1 &= z_2, \\ \dot{z}_2 &= -z_2 z_4, \\ \dot{z}_3 &= z_2 z_3, \\ \dot{z}_4 &= 2 z_2 \dot{z}_2 z_3 + z_2^2 \dot{z}_3 = -2 z_4^2 + z_2 z_4,\end{aligned}$$

which is a quadratic model of the form (2).  $\triangle$

In what follows, we assume that the original state space variables  $x_1, \dots, x_n$  can be written as linear combinations of the feature space variables  $z_1, \dots, z_N$ , which implies that there exists a matrix  $G \in \mathbb{R}^{n \times N}$  such that

$$x = Gz.$$

This is similar to the assumption that the so-called full-state observable  $g(x) = x$ , which for Koopman operator-based methods such as EDMD and gEDMD is required for the decomposition of the dynamics into eigenvalues, eigenfunctions, and modes, is contained in the span of the basis functions, see [5, 12] for details. The easiest way to accomplish this is to add the observables  $\{x_i\}_{i=1}^n$  to the dictionary. The above assumption then implies that

$$\dot{x} = G\dot{z} = GA(z \otimes z) + GBz + GC. \quad (3)$$

That is, once we have learned the quadratic embedding, we can also extract the governing equations of the original dynamical system. Note that after mapping the initial condition  $x(t_0) = x_0$  to the feature space using  $z(t_0) = \phi(x_0)$ , we do not need to evaluate the typically nonlinear functions contained in the dictionary anymore.

**Example 2.3.** Let us consider two simple guiding examples:

i) Given  $\dot{x} = -\frac{x}{1+x}$ , see [28], we define

$$z = \begin{bmatrix} x \\ \frac{1}{1+x} \\ \frac{x}{(1+x)^2} \end{bmatrix} \implies \dot{z} = \begin{bmatrix} 1 \\ -\frac{1}{(1+x)^2} \\ \frac{1}{(1+x)^2} - \frac{2x}{(1+x)^3} \end{bmatrix} \left( -\frac{x}{1+x} \right) = \begin{bmatrix} -z_1 z_2 \\ z_2 z_3 \\ -z_2 z_3 + 2z_3^2 \end{bmatrix},$$

so that in this case  $G = [1 \ 0 \ 0]$ . We can rewrite the nonlinear system as a quadratic differential equation of the form (2) in a three-dimensional space, with

$$A = \begin{bmatrix} z_1^2 & z_1 z_2 & z_1 z_3 & z_2 z_1 & z_2^2 & z_2 z_3 & z_3 z_1 & z_3 z_2 & z_3^2 \\ 0 & -1 & 0 & 0 & 0 & 0 & 0 & 0 & 0 \\ 0 & 0 & 0 & 0 & 0 & 1 & 0 & 0 & 0 \\ 0 & 0 & 0 & 0 & 0 & -1 & 0 & 0 & 2 \end{bmatrix}, \quad B = \begin{bmatrix} z_1 & z_2 & z_3 \\ 0 & 0 & 0 \\ 0 & 0 & 0 \\ 0 & 0 & 0 \end{bmatrix}, \quad C = \begin{bmatrix} 1 \\ 0 \\ 0 \\ 0 \end{bmatrix}.$$

As already mentioned above, this representation is in general not unique, even if we remove the redundant columns from the matrix  $A$ . We could, for instance, also write  $\dot{z}_1 = -z_1 z_3 - z_3$  or use any convex combination of the two corresponding matrix representations.

ii) For the damped nonlinear pendulum, see also [28], given by

$$\begin{bmatrix} \dot{x}_1 \\ \dot{x}_2 \end{bmatrix} = \begin{bmatrix} x_2 \\ -\sin(x_1) - cx_2 \end{bmatrix},$$

where  $c$  is the damping constant, we define

$$z = \begin{bmatrix} x_1 \\ x_2 \\ \sin(x_1) \\ \cos(x_1) \end{bmatrix} \implies \dot{z} = \begin{bmatrix} 1 & 0 \\ 0 & 1 \\ \cos(x_1) & 0 \\ -\sin(x_1) & 0 \end{bmatrix} \begin{bmatrix} x_2 \\ -\sin(x_1) - cx_2 \end{bmatrix} = \begin{bmatrix} z_2 \\ -z_3 - cz_2 \\ z_2 z_4 \\ -z_2 z_3 \end{bmatrix}.$$

The projection onto the original state space is then defined by the matrix

$$G = \begin{bmatrix} 1 & 0 & 0 & 0 \\ 0 & 1 & 0 & 0 \end{bmatrix}.$$

This shows that we can represent the nonlinear pendulum by a quadratic system in a four-dimensional space.  $\triangle$

**Remark 2.4.** The quadratic embedding approach is similar to the Koopman linearization, which seeks to find a linear but in general infinite-dimensional representation of the system:

i) First, consider

$$\begin{bmatrix} \dot{x}_1 \\ \dot{x}_2 \end{bmatrix} = \begin{bmatrix} x_1 - x_2^4 \\ 2x_2 \end{bmatrix}.$$

Defining  $z_1 = x_1$ ,  $z_2 = x_2$ , and  $z_3 = x_2^4$ , i.e.,  $\phi(x) = [x_1, x_2, x_2^4]^\top$ , we can rewrite the nonlinear system as a linear system

$$\begin{bmatrix} \dot{z}_1 \\ \dot{z}_2 \\ \dot{z}_3 \end{bmatrix} = \begin{bmatrix} 1 & 0 & -1 \\ 0 & 2 & 0 \\ 0 & 0 & 8 \end{bmatrix} \begin{bmatrix} z_1 \\ z_2 \\ z_3 \end{bmatrix}$$

in three dimensions. The three observables  $\phi_i$ ,  $i = 1, \dots, 3$ , span in this case an invariant subspace of the Koopman generator associated with the original nonlinear system. Given a linear dynamical system  $\dot{z} = Bz$ , we can construct eigenfunctions of the Koopman generator by computing left eigenvectors of the matrix  $B$ . Assume that  $B^\top v = \lambda v$ , then  $\varphi(z) = z \cdot v$  is an eigenfunction since

$$\mathcal{L}\varphi(z) = (Bz) \cdot v = z \cdot (B^\top v) = z \cdot (\lambda v) = \lambda \varphi(z).$$

Products of these eigenfunctions are again eigenfunctions. We can use this approach to compute eigenfunctions of the original system. For the above system, for instance, we obtain the eigenfunction  $\varphi(x) = 7x_1 + x_2^4$ . In general, however, the projection of the Koopman generator onto a finite-dimensional subspace spanned by a set of basis functions leads to approximation errors, see [12] for details.

ii) For the modified system

$$\begin{bmatrix} \dot{x}_1 \\ \dot{x}_2 \end{bmatrix} = \begin{bmatrix} x_1 - x_2^4 \\ x_1 + 2x_2 \end{bmatrix},$$

on the other hand, this linearization approach does not work: Defining again  $z_1 = x_1$ ,  $z_2 = x_2$ , and  $z_3 = x_2^4$ , we have  $\dot{z}_3 = 4z_1 z_2^3 + 8z_3$ , which would require introducing a new auxiliary variable  $z_4 = z_1 z_2^3$  so that  $\dot{z}_4 = z_4 - z_2^7 + 3z_1^2 + 3z_1 z_2$ , which in turn would again require defining new variables. In this case, we would need infinitely many terms. In order to find a quadratic model, we can simply define

$$z = \begin{bmatrix} x_1 \\ x_2 \\ x_2^2 \end{bmatrix} \implies \dot{z} = \begin{bmatrix} z_1 - z_3^2 \\ z_1 + 2z_2 \\ 2z_1 z_2 + 4z_3 \end{bmatrix},$$

i.e., the system is quadratic in the chosen three-dimensional feature space.  $\triangle$

The example illustrates that if we add new variables and apply the chain rule to derive a linear model, this process does in general not terminate. If we allow quadratic systems, on the other hand, it is always possible to determine a finite-dimensional model [18, 19].

### 3. Learning quadratic embeddings from data

Our goal is to learn the quadratic embedding (2) from simulation or measurement data. Assume we have  $m$  data points  $x^{(k)}$ , extracted for instance from one long trajectory, and the corresponding time derivatives  $\dot{x}^{(k)}$ . Our training data is thus given by  $\{(x^{(k)}, \dot{x}^{(k)})\}_{k=1}^m$ . We either need to be able to evaluate the right-hand side pointwise to compute  $\dot{x}^{(k)} = F(x^{(k)})$  or estimate the derivatives using finite difference approximations. In addition to the training data, we have to select a set of basis functions  $\{\phi_1, \dots, \phi_N\}$ . The gradients of the basis functions, which will be required later, can be computed analytically or using automatic differentiation.

#### 3.1. Derivation of QENDy

Let  $z^{(k)} = \phi(x^{(k)})$  and  $\dot{z}^{(k)} = J(x^{(k)})\dot{x}^{(k)}$ . In order to find the optimal  $A$ ,  $B$ , and  $C$  in (2) for the given set of basis functions, we minimize the loss function

$$L(A, B, C) = \sum_{k=1}^m \left\| \dot{z}^{(k)} - A(z^{(k)} \otimes z^{(k)}) - Bz^{(k)} - C \right\|_2^2.$$

We define the data matrices

$$\begin{aligned} Z_1 &= [z^{(1)} \quad z^{(2)} \quad \dots \quad z^{(m)}] \in \mathbb{R}^{N \times m}, \\ Z_2 &= [z^{(1)} \otimes z^{(1)} \quad z^{(2)} \otimes z^{(2)} \quad \dots \quad z^{(m)} \otimes z^{(m)}] \in \mathbb{R}^{N^2 \times m}, \\ \dot{Z} &= [\dot{z}^{(1)} \quad \dot{z}^{(2)} \quad \dots \quad \dot{z}^{(m)}] \in \mathbb{R}^{N \times m}, \end{aligned}$$

so that we can rewrite the loss function as

$$L(A, B, C) = \left\| \dot{Z} - AZ_2 - BZ_1 - C\mathbf{1}_m^\top \right\|_F^2, \quad (4)$$

where  $\|\cdot\|_F$  denotes the Frobenius norm and  $\mathbf{1}_m \in \mathbb{R}^m$  the vector of ones, which is here simply used to create  $m$  copies of the vector  $C$ .

**Theorem 3.1.** *The derivatives of the loss function (4) with respect to  $A$ ,  $B$ , and  $C$  are given by*

$$\begin{aligned} \frac{\partial L(A, B, C)}{\partial A} &= 2AZ_2Z_2^\top - 2\dot{Z}Z_2^\top + 2BZ_1Z_2^\top + 2C\mathbf{1}_m^\top Z_2^\top, \\ \frac{\partial L(A, B, C)}{\partial B} &= 2BZ_1Z_1^\top - 2\dot{Z}Z_1^\top + 2AZ_2Z_1^\top + 2C\mathbf{1}_m^\top Z_1^\top, \\ \frac{\partial L(A, B, C)}{\partial C} &= 2mC - 2\dot{Z}\mathbf{1}_m + 2AZ_2\mathbf{1}_m + 2BZ_1\mathbf{1}_m. \end{aligned}$$

*Proof.* We first rewrite the loss function as

$$\begin{aligned} L(A, B, C) &= \left\| \dot{Z} - AZ_2 - BZ_1 - C\mathbf{1}_m^\top \right\|_F^2 \\ &= \underbrace{\text{tr}(\dot{Z}^\top \dot{Z})}_{\textcircled{0}} + \underbrace{\text{tr}(Z_2^\top A^\top A Z_2)}_{\textcircled{1}} + \underbrace{\text{tr}(Z_1^\top B^\top B Z_1)}_{\textcircled{2}} + \underbrace{\text{tr}(\mathbf{1}_m C^\top C \mathbf{1}_m^\top)}_{\textcircled{3}} \\ &\quad - \underbrace{2 \text{tr}(\dot{Z}^\top A Z_2)}_{\textcircled{4}} - \underbrace{2 \text{tr}(\dot{Z}^\top B Z_1)}_{\textcircled{5}} - \underbrace{2 \text{tr}(\dot{Z}^\top C \mathbf{1}_m^\top)}_{\textcircled{6}} \\ &\quad + \underbrace{2 \text{tr}(Z_2^\top A^\top B Z_1)}_{\textcircled{7}} + \underbrace{2 \text{tr}(Z_2^\top A^\top C \mathbf{1}_m^\top)}_{\textcircled{8}} + \underbrace{2 \text{tr}(Z_1^\top B^\top C \mathbf{1}_m^\top)}_{\textcircled{9}}. \end{aligned}$$

Let us now compute the derivatives with respect to the matrix  $A$ . Only the terms ①, ④, ⑦, and ⑧ depend on  $A$ . It holds that

$$\frac{\partial}{\partial A} \operatorname{tr}(XAY) = X^\top Y^\top \quad \text{and} \quad \frac{\partial}{\partial A} \operatorname{tr}(A^\top XAY) = XAY + X^\top AY^\top,$$

see, e.g., [34]. For term ①, using the cyclic property of the trace, this implies

$$\frac{\partial}{\partial A} \operatorname{tr}(Z_2^\top A^\top AZ_2) = \frac{\partial}{\partial A} \operatorname{tr}(A^\top AZ_2Z_2^\top) = 2AZ_2Z_2^\top.$$

Similarly, for the terms ④, ⑦, and ⑧, we obtain

$$\begin{aligned} \frac{\partial}{\partial A} \operatorname{tr}(\dot{Z}^\top AZ_2) &= \dot{Z}Z_2^\top, \\ \frac{\partial}{\partial A} \operatorname{tr}(Z_2^\top A^\top BZ_1) &= BZ_1Z_2^\top, \\ \frac{\partial}{\partial A} \operatorname{tr}(Z_2^\top A^\top C\mathbf{1}_m^\top) &= C\mathbf{1}_m^\top Z_2^\top, \end{aligned}$$

where we used  $\operatorname{tr}(X) = \operatorname{tr}(X^\top)$ . The derivatives with respect to  $B$  follow in an analogous fashion. Finally, we compute the derivatives with respect to  $C$ . For term ③, we get

$$\frac{\partial}{\partial C} \operatorname{tr}(\mathbf{1}_m C^\top C \mathbf{1}_m^\top) = \frac{\partial}{\partial C} \operatorname{tr}(\mathbf{1}_m^\top \mathbf{1}_m C^\top C) = m \frac{\partial}{\partial C} \operatorname{tr}(C^\top C) = 2mC.$$

The remaining derivatives for the terms ⑥, ⑧, and ⑨ can be computed in the same way.  $\square$

In order to find an optimal solution, the derivatives in Theorem 3.1 must be zero. Transposing the equations, we obtain

$$\begin{aligned} Z_2 Z_2^\top A^\top + Z_2 Z_1^\top B^\top + Z_2 \mathbf{1}_m C^\top &= Z_2 \dot{Z}^\top, \\ Z_1 Z_2^\top A^\top + Z_1 Z_1^\top B^\top + Z_1 \mathbf{1}_m C^\top &= Z_1 \dot{Z}^\top, \\ \mathbf{1}_m^\top Z_2^\top A^\top + \mathbf{1}_m^\top Z_1^\top B^\top + m C^\top &= \mathbf{1}_m^\top \dot{Z}^\top. \end{aligned} \tag{5}$$

**Definition 3.2** (Vectorization). *Let  $X \in \mathbb{R}^{m \times n}$  be an arbitrary matrix. We define  $\operatorname{vec}(X) \in \mathbb{R}^{mn}$  to be the vectorization of  $X$ , which reshapes a matrix as a vector by stacking its columns.*

**Lemma 3.3.** *Given two matrices  $X \in \mathbb{R}^{m \times n}$  and  $Y \in \mathbb{R}^{n \times \ell}$ , it holds that*

$$\operatorname{vec}(XY) = (I_\ell \otimes X) \operatorname{vec}(Y) \in \mathbb{R}^{m\ell},$$

see, e.g., [34].

As a result, we can rewrite (5) as a system of linear equations

$$\left[ \begin{array}{c|c|c} I_N \otimes (Z_2 Z_2^\top) & I_N \otimes (Z_2 Z_1^\top) & I_N \otimes (Z_2 \mathbf{1}_m) \\ \hline I_N \otimes (Z_1 Z_2^\top) & I_N \otimes (Z_1 Z_1^\top) & I_N \otimes (Z_1 \mathbf{1}_m) \\ \hline I_N \otimes (\mathbf{1}_m^\top Z_2^\top) & I_N \otimes (\mathbf{1}_m^\top Z_1^\top) & m I_N \end{array} \right] \begin{bmatrix} \operatorname{vec}(A^\top) \\ \operatorname{vec}(B^\top) \\ \operatorname{vec}(C^\top) \end{bmatrix} = \begin{bmatrix} \operatorname{vec}(Z_2 \dot{Z}^\top) \\ \operatorname{vec}(Z_1 \dot{Z}^\top) \\ \operatorname{vec}(\mathbf{1}_m^\top \dot{Z}^\top) \end{bmatrix}$$

of size  $N^3 + N^2 + N$ . Note, however, that the system can be decoupled into  $N$  systems of size  $N^2 + N + 1$ . Let  $A_\ell$ ,  $B_\ell$ , and  $\dot{Z}_\ell$  denote the  $\ell$ th rows of the matrices  $A$ ,  $B$ , and  $\dot{Z}$ , respectively, and let  $C_\ell$  be the  $\ell$ th entry of the vector  $C$ . We can then solve

$$\underbrace{\left[ \begin{array}{c|c|c} Z_2 Z_2^\top & Z_2 Z_1^\top & Z_2 \mathbf{1}_m \\ \hline Z_1 Z_2^\top & Z_1 Z_1^\top & Z_1 \mathbf{1}_m \\ \hline \mathbf{1}_m^\top Z_2^\top & \mathbf{1}_m^\top Z_1^\top & m \end{array} \right]}_R \underbrace{\begin{bmatrix} A_\ell^\top \\ B_\ell^\top \\ C_\ell \end{bmatrix}}_{v_\ell} = \underbrace{\begin{bmatrix} Z_2 \dot{Z}_\ell^\top \\ Z_1 \dot{Z}_\ell^\top \\ \mathbf{1}_m^\top \dot{Z}_\ell^\top \end{bmatrix}}_{s_\ell} \tag{6}$$

for  $\ell = 1, \dots, N$ . Since the quadratic embedding is in general not unique—even if we eliminate the redundant columns of the matrix  $A$ —as shown in Example 2.3, the matrix  $R$  is not necessarily invertible so that we define  $v_\ell = R^+ s_\ell$ , where  $R^+$  denotes the pseudoinverse of the symmetric matrix  $R$ . That is,  $v_\ell$  is the solution with the smallest 2-norm. Solving the  $N$  systems of equations allows us to compute  $A$ ,  $B$ , and  $C$  row-wise. We call this method *QENDy*.

**Example 3.4.** Let us consider the systems along with the dictionaries defined in Example 2.3:

- i) We generate eleven training data points by simulating the rational system for  $t \in [0, 5]$  using the initial condition  $x(0) = 1$ . To avoid too many redundant solutions, we set  $C = 0$ . Applying QENDy then yields

$$\dot{z} = \begin{bmatrix} -0.7 z_1 z_2 - 0.3 z_1 z_3 + 0.1 z_2^2 - 0.1 z_2 - 0.2 z_3 \\ z_2 z_3 \\ -z_2 z_3 + 2 z_3^2 \end{bmatrix} \implies \dot{x} = -\frac{x}{1+x}.$$

We obtain a valid quadratic embedding and can also identify the governing equations (after simplifying the right-hand side) using (3). It would be possible to represent  $\dot{z}_1$  using fewer terms, this could be accomplished by adding sparsity constraints to the loss function.

- ii) For the nonlinear damped pendulum, we choose the damping coefficient  $c = 0.1$ . Even when the number of training data points is small, QENDy returns

$$\dot{z} = \begin{bmatrix} z_2 \\ -0.1 z_2 - z_3 \\ z_2 z_4 \\ -z_2 z_3 \end{bmatrix} \implies \dot{x} = \begin{bmatrix} x_2 \\ -0.1 x_2 - \sin(x_1) \end{bmatrix}.$$

The convergence will be analyzed in more detail in Example 3.5. △

In general, we do not know the feature space mapping that results in a perfect quadratic embedding of the dynamics, but we will nevertheless obtain the best approximation for a given set of basis functions and training data points as we will show next. One of the main advantages of QENDy, compared to deep learning methods, is that it generalizes well to unseen data and also allows us to explicitly write the governing equations in terms of the basis functions.

### 3.2. Convergence of QENDy

Let us now analyze the convergence of QENDy in the infinite data limit, assuming that the training data points  $x^{(k)}$  are sampled from a (potentially unknown) distribution  $\mu$ . In order to compute the  $\ell$ th rows of  $A$ ,  $B$ , and  $C$ , we have to solve the system of linear equations (6). First, we divide both sides by the number of data points  $m$ . Let  $(i, j) \mapsto \overline{ij} := N(j-1) + i$  be the canonical mapping from  $\{1, \dots, N\} \times \{1, \dots, N\}$  to  $\{1, \dots, N^2\}$ , then

$$\frac{1}{m} Z_2 Z_2^\top = \frac{1}{m} \sum_{k=1}^m (z^{(k)} \otimes z^{(k)}) (z^{(k)} \otimes z^{(k)})^\top$$

and the entry in row  $\overline{i_1 i_2}$  and column  $\overline{j_1 j_2}$  is

$$\begin{aligned} \left[ \frac{1}{m} Z_2 Z_2^\top \right]_{\overline{i_1 i_2} \overline{j_1 j_2}} &= \frac{1}{m} \sum_{k=1}^m z_{i_1}^{(k)} z_{i_2}^{(k)} z_{j_1}^{(k)} z_{j_2}^{(k)} = \frac{1}{m} \sum_{k=1}^m \phi_{i_1}(x^{(k)}) \phi_{i_2}(x^{(k)}) \phi_{j_1}(x^{(k)}) \phi_{j_2}(x^{(k)}) \\ &\xrightarrow{m \rightarrow \infty} \int \phi_{i_1}(x) \phi_{i_2}(x) \phi_{j_1}(x) \phi_{j_2}(x) d\mu(x) = \langle \phi_{i_1} \phi_{i_2}, \phi_{j_1} \phi_{j_2} \rangle_\mu. \end{aligned}$$



Analogously, we obtain

$$\begin{aligned} \left[ \frac{1}{m} Z_2 Z_1^\top \right]_{\overline{i_1 i_2} j} &\xrightarrow{m \rightarrow \infty} \langle \phi_{i_1} \phi_{i_2}, \phi_j \rangle_\mu, & \left[ \frac{1}{m} Z_2 \mathbf{1}_m \right]_{\overline{i_1 i_2}} &\xrightarrow{m \rightarrow \infty} \langle \phi_{i_1} \phi_{i_2}, \mathbf{1} \rangle_\mu, \\ \left[ \frac{1}{m} Z_1 Z_1^\top \right]_{ij} &\xrightarrow{m \rightarrow \infty} \langle \phi_i, \phi_j \rangle_\mu, & \left[ \frac{1}{m} Z_1 \mathbf{1}_m \right]_i &\xrightarrow{m \rightarrow \infty} \langle \phi_i, \mathbf{1} \rangle_\mu, \end{aligned}$$

where  $\mathbf{1}(x) \equiv 1$  is the constant one function. For the right-hand side, we have

$$\left[ \frac{1}{m} Z_2 \dot{Z}_\ell^\top \right]_{\overline{i_1 i_2}} \xrightarrow{m \rightarrow \infty} \langle \phi_{i_1} \phi_{i_2}, \dot{z}_\ell \rangle_\mu = \langle \phi_{i_1} \phi_{i_2}, \nabla \phi_\ell \cdot F \rangle_\mu,$$

and similarly

$$\left[ \frac{1}{m} Z_1 \dot{Z}_\ell^\top \right]_i \xrightarrow{m \rightarrow \infty} \langle \phi_i, \nabla \phi_\ell \cdot F \rangle_\mu, \quad \frac{1}{m} \mathbf{1}_m^\top \dot{Z}_\ell^\top \xrightarrow{m \rightarrow \infty} \langle \mathbf{1}, \nabla \phi_\ell \cdot F \rangle_\mu.$$

Overall, this results in the system of linear equations

$$\underbrace{\begin{bmatrix} \langle \phi_{i_1} \phi_{i_2}, \phi_{j_1} \phi_{j_2} \rangle_\mu & \langle \phi_{i_1} \phi_{i_2}, \phi_j \rangle_\mu & \langle \phi_{i_1} \phi_{i_2}, \mathbf{1} \rangle_\mu \\ \langle \phi_i, \phi_{j_1} \phi_{j_2} \rangle_\mu & \langle \phi_i, \phi_j \rangle_\mu & \langle \phi_i, \mathbf{1} \rangle_\mu \\ \langle \mathbf{1}, \phi_{j_1} \phi_{j_2} \rangle_\mu & \langle \mathbf{1}, \phi_j \rangle_\mu & \langle \mathbf{1}, \mathbf{1} \rangle_\mu \end{bmatrix}}_{R^*} \underbrace{\begin{bmatrix} A_\ell^\top \\ B_\ell^\top \\ C_\ell \end{bmatrix}}_{v_\ell^*} = \underbrace{\begin{bmatrix} \langle \phi_{i_1} \phi_{i_2}, \nabla \phi_\ell \cdot F \rangle \\ \langle \phi_i, \nabla \phi_\ell \cdot F \rangle \\ \langle \mathbf{1}, \nabla \phi_\ell \cdot F \rangle \end{bmatrix}}_{s_\ell^*}.$$

In the infinite data limit, we can thus view QENDy as  $N$  continuous best approximations of  $\nabla \phi_\ell \cdot F$ , where  $\ell = 1, \dots, N$ , with respect to the  $\mu$ -weighted inner product using the (linearly dependent) basis functions

$$\{\phi_{i_1} \phi_{i_2}\}_{i_1, i_2=1}^N \cup \{\phi_i\}_{i=1}^N \cup \{\mathbf{1}\},$$

which we will call the *quadratically augmented basis* in what follows. The corresponding augmented feature map will be denoted by  $\bar{\phi}: \mathbb{R}^n \rightarrow \mathbb{R}^{N^2+N+1}$ . QENDy itself is a discrete best approximation. More details about discrete and continuous best approximation problems can be found in Appendix A.

**Example 3.5.** In order to corroborate the above convergence results, let us consider again the damped pendulum and generate  $m$  uniformly distributed (since this simplifies the convergence analysis) training data points  $x^{(k)}$  in  $[-1, 1] \times [-1, 1]$ , for which we then compute the exact derivatives  $\dot{x}^{(k)}$ . Using the feature space mapping described in Example 2.3, we compute the matrix  $R$  and the vectors  $s_\ell$  using QENDy and  $R^*$  and  $s_\ell^*$  by computing the required integrals analytically. We then compare the entries element-wise and calculate the mean difference averaged over 100 runs. Additionally, we simulate the identified models for  $m = 6$ ,  $m = 8$ , and  $m = 10$  and compare the trajectories with the true solution. The results, shown in Figure 1, illustrate that QENDy indeed converges to the best approximation and that the identified models are good approximations of the true dynamics, even for small values of  $m$ .  $\triangle$

### 3.3. Regularization and stability

For autonomous quadratic systems, i.e.,  $C = 0$  in (2), the stability radius of the equilibrium at the origin is inversely proportional to the norm of the matrix  $A$ . This result relies on Lyapunov stability theory and requires that the matrix  $B$  is Hurwitz stable, i.e., all the eigenvalues of  $B$  have negative real parts [35, 36]. The latter condition ensures that the origin is locally asymptotically stable in the first place. The paper [36] extends this result to cubic systems and leverages it to propose a

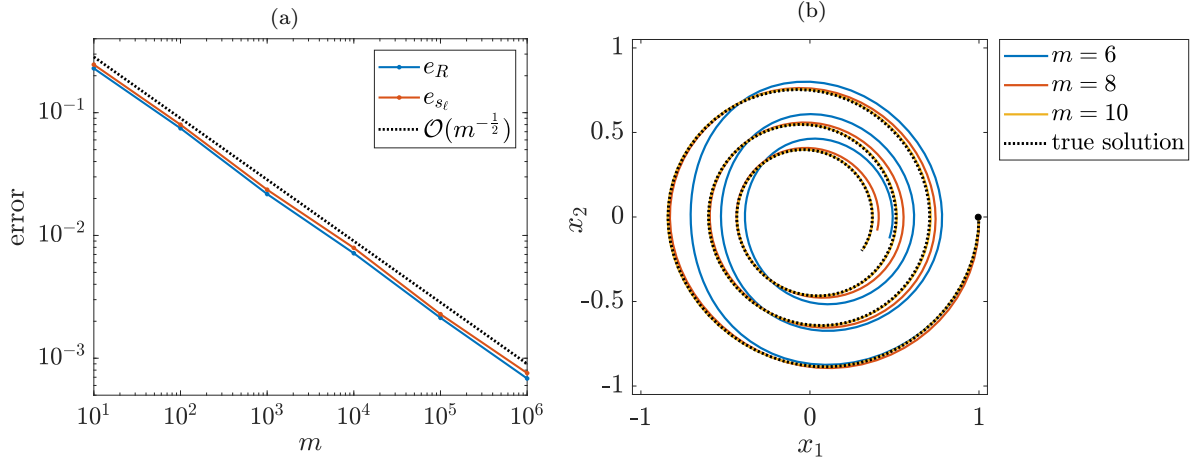


**Figure 1:** (a) Average difference between the entries of  $R$  and  $R^*$  (denoted by  $e_R$ ) as well as  $s_\ell$  and  $s_\ell^*$  (denoted by  $e_{s_\ell}$ ) as a function of the number of training data points  $m$ , illustrating the expected  $\mathcal{O}(m^{-\frac{1}{2}})$  Monte Carlo convergence. (b) Simulation of the learned quadratic models for  $m = 6$ ,  $m = 8$ , and  $m = 10$ . The black dot represents the initial condition  $x = [1, 0]^\top$ .

regularization of the operator inference method [30] for non-intrusive reduced-order modeling that promotes models with a large stability radius by penalizing the Frobenius norms of the learned quadratic and cubic operators. This regularization does, however, not guarantee that the learned matrix  $B$  is Hurwitz stable. Instead, it relies on an eigen-reflection post-processing step to enforce Hurwitz stability.

Hurwitz stability of the matrix  $B$  can be incorporated into the optimization process to learn quadratic models that are stable by design by exploiting the fact that any Hurwitz stable matrix  $B$  can be written as a product of generalized negative definite matrix  $P$  and a symmetric positive definite matrix  $Q$  [37]. This idea is leveraged in [38] and applied to the operator inference method and SINDy, where in particular the parametrization

$$P = (J - J^T) - RR^\top, \quad \text{and} \quad Q = LL^\top$$

is used. Here,  $J$ ,  $R$ , and  $L$  are general matrices of the same dimensions as  $B$ , which ensures that  $Q$  is semi-positive definite only. It is important to note, however, that the resulting optimization problem is non-convex and can only be solved using iterative methods, whereas the  $\|A\|_F$ -penalized operator inference optimization problem can be solve analytically.

In this work, we follow the same approach as in [36] to promote stability in models learned by QENDy. In particular, we modify the loss function (4) as follows:

$$L(A, B, C) = \left\| \dot{Z} - AZ_2 - BZ_1 - C\mathbf{1}_m^\top \right\|_F^2 + \lambda \|A\|_F^2, \quad (7)$$

where  $\lambda \geq 0$  is a regularization parameter. Following the same approach as in Section 3.1, we obtain the system of linear equations

$$\underbrace{\begin{bmatrix} Z_2 Z_2^\top + \lambda I_N & Z_2 Z_1^\top & Z_2 \mathbf{1}_m \\ Z_1 Z_2^\top & Z_1 Z_1^\top & Z_1 \mathbf{1}_m \\ \mathbf{1}_m^\top Z_2^\top & \mathbf{1}_m^\top Z_1^\top & m \end{bmatrix}}_{R_\lambda} \underbrace{\begin{bmatrix} A_\ell^\top \\ B_\ell^\top \\ C_\ell \end{bmatrix}}_{v_\ell} = \underbrace{\begin{bmatrix} Z_2 \dot{Z}_\ell^\top \\ Z_1 \dot{Z}_\ell^\top \\ \mathbf{1}_m^\top \dot{Z}_\ell^\top \end{bmatrix}}_{s_\ell}, \quad (8)$$

which we solve to obtain  $v_\ell = R_\lambda^+ s_\ell$ .

### 3.4. Comparison with SINDy

Let us compare QENDy with the well-known method SINDy [29]. Although the original SINDy formulation was limited to ordinary differential equations, similar methods have been developed for stochastic differential equations [39] and partial differential equations [40]. Given again training data of the form  $\{(x^{(k)}, \dot{x}^{(k)})\}_{k=1}^m$  and a set of basis functions  $\{\phi_1, \dots, \phi_N\}$ , we define

$$\begin{aligned}\Phi_X &= [\phi(x^{(1)}) \quad \phi(x^{(2)}) \quad \dots \quad \phi(x^{(m)})] \in \mathbb{R}^{N \times m}, \\ \dot{X} &= [\dot{x}^{(1)} \quad \dot{x}^{(2)} \quad \dots \quad \dot{x}^{(m)}] \in \mathbb{R}^{n \times m},\end{aligned}$$

i.e.,  $\Phi_X = Z_1$ . The SINDy loss function is then given by

$$L(\Xi) = \left\| \dot{X} - \Xi \Phi_X \right\|_F^2,$$

where  $\Xi \in \mathbb{R}^{n \times N}$ . In addition to minimizing the regression error, it is also possible to penalize non-sparse solutions  $\Xi$  in order to find models that are as simple as possible. The identified system is then defined by the optimal solution  $\Xi$  that minimizes the loss function, i.e.,

$$\dot{x} = \Xi \phi(x).$$

Neglecting the sparsity constraints and following the same steps as above, we obtain the system of equations

$$\Phi_X \Phi_X^\top \Xi^\top = \Phi_X \dot{X}^\top,$$

which we decouple into  $n$  problems of the form

$$\Phi_X \Phi_X^\top \Xi_\ell^\top = \Phi_X \dot{X}_\ell^\top,$$

where  $\Xi_\ell$  and  $\dot{X}_\ell$  denote the  $\ell$ th rows of  $\Xi$  and  $\dot{X}$ , respectively. Dividing again both sides by the number of data points  $m$  and letting  $m$  go to infinity yields

$$\begin{aligned}\left[ \frac{1}{m} \Phi_X \Phi_X^\top \right]_{ij} &\xrightarrow{m \rightarrow \infty} \langle \phi_i, \phi_j \rangle_\mu, \\ \left[ \frac{1}{m} \Phi_X \dot{X}_\ell^\top \right]_i &\xrightarrow{m \rightarrow \infty} \langle \phi_i, F_\ell \rangle_\mu.\end{aligned}$$

That is, in the infinite data limit we are solving the system of equations

$$\left[ \langle \phi_i, \phi_j \rangle_\mu \right] \Xi_\ell^\top = \left[ \langle \phi_i, F_\ell \rangle_\mu \right]$$

for  $\ell = 1, \dots, n$  in the least-squares sense. This illustrates that SINDy is a data-driven best approximation of  $F$  using the basis functions  $\{\phi_i\}_{i=1}^N$ .

**Remark 3.6.** Using properties of the pseudoinverse, we could have also directly written

$$\Xi = \dot{X} \Phi_X^+ = (\dot{X} \Phi_X^\top) (\Phi_X \Phi_X^\top)^+,$$

which results in the same system of equations. Our goal, however, was to highlight similarities with the quadratic embedding.

**Example 3.7.** Let us consider the simple systems defined in Example 2.3:

- i) SINDy would not be able to find the governing equations of the rational system using the three selected basis functions since the right-hand side cannot be represented by a linear combination of these functions, but we would obtain an approximation of the dynamics.

ii) The governing equations of the nonlinear pendulum, on the other hand, can be identified using SINDy with the chosen dictionary. In this case, we obtain

$$\dot{x} = \underbrace{\begin{bmatrix} 0 & 1 & 0 & 0 \\ 0 & -0.1 & -1 & 0 \end{bmatrix}}_{\Xi} \begin{bmatrix} x_1 \\ x_2 \\ \sin(x_1) \\ \cos(x_1) \end{bmatrix}. \quad \triangle$$

It would of course also be possible to use SINDy along with the quadratically augmented basis.

### 3.5. Comparison with gEDMD

There are also closely related methods for learning the governing equations that are based on the Koopman generator [9, 12]. We will now compare QENDy and gEDMD [12], which aims at approximating the Koopman generator associated with ordinary or stochastic differential equations. Let  $\dot{\phi}(x) = (\mathcal{L}\phi)(x) = J(x)F(x)$ , where the Koopman generator associated with (1) is again applied component-wise. We define the matrices

$$\begin{aligned} \Phi_X &= [\phi(x^{(1)}) \quad \phi(x^{(2)}) \quad \dots \quad \phi(x^{(m)})] \in \mathbb{R}^{N \times m}, \\ \dot{\Phi}_X &= [\dot{\phi}(x^{(1)}) \quad \dot{\phi}(x^{(2)}) \quad \dots \quad \dot{\phi}(x^{(m)})] \in \mathbb{R}^{N \times m}. \end{aligned}$$

The loss function is in this case defined by

$$L(\Theta) = \left\| \dot{\Phi}_X - \Theta \Phi_X \right\|_F^2.$$

Setting the derivative of the loss function with respect to the matrix  $\Theta$  to zero results in the system of equations

$$\Phi_X \Phi_X^\top \Theta^\top = \Phi_X \dot{\Phi}_X^\top.$$

In the infinite data limit, we obtain

$$\begin{aligned} \left[ \frac{1}{m} \Phi_X \Phi_X^\top \right]_{ij} &\xrightarrow{m \rightarrow \infty} \langle \phi_i, \phi_j \rangle_\mu, \\ \left[ \frac{1}{m} \Phi_X \dot{\Phi}_X^\top \right]_{ij} &\xrightarrow{m \rightarrow \infty} \langle \phi_i, \mathcal{L}\phi_j \rangle_\mu, \end{aligned}$$

so that  $\Theta^\top$  can be regarded as the matrix representation of the Koopman generator projected onto the space spanned by the basis functions  $\phi$ . In other words, gEDMD computes a Galerkin approximation of the operator  $\mathcal{L}$ , where the required integrals are estimated from data. Given a function  $f(x) = \alpha^\top \phi(x)$ , we have

$$\mathcal{L}f(x) \approx \alpha^\top \Theta \phi(x).$$

For the full-state observable  $g(x) = x = G\phi(x)$ , this implies

$$\dot{x} = F(x) = \mathcal{L}g(x) \approx G\Theta\phi(x) = \Xi\phi(x),$$

which shows that gEDMD can be used for system identification, see [12] for details. However, gEDMD also works for stochastic differential equations and allows us to compute spectral properties of the Koopman generator and to decompose the right-hand side  $F$  into eigenvalues, eigenfunctions, and associated modes. To demonstrate that QENDy and gEDMD are related as well, we now approximate the Koopman generator using the augmented basis given by  $\bar{\phi}$ . It then holds that  $R = \bar{\Phi}_X \bar{\Phi}_X^\top$  and  $s_\ell$  is the  $(N^2 + \ell)$ th column of the matrix  $\bar{\Phi}_X \dot{\bar{\Phi}}_X^\top$ . The Koopman generator approximation with respect to the quadratically augmented basis contains more information about the system, namely the action of the Koopman generator applied to products of basis functions.

### 3.6. Comparison with quadratic embeddings using deep learning

QENDy uses a dictionary containing a predefined set of basis functions to map a nonlinear dynamical system to an embedding space where the dynamics can be expressed in a quadratic form, either exactly or approximately. A different approach, proposed in [28], is to define an embedding map,  $x \mapsto z = \phi_{w_{\text{enc}}}(x)$ , using an encoder neural network and to reconstruct  $x$  from  $z$  using a decoder neural network,  $z \mapsto x = \psi_{w_{\text{dec}}}(z)$ . The goal is then to optimize the parameters  $w_{\text{enc}}$  and  $w_{\text{dec}}$  of the encoder and decoder and, at the same time,  $A$ ,  $B$ , and  $C$  such that  $z$  satisfies (2) as well as the encoder–decoder property  $\psi_{w_{\text{dec}}}(\phi_{w_{\text{enc}}}(x)) = x$ . This leads to the following loss functions that need to be optimized simultaneously:

i) Encoder–decoder reconstruction:

$$\mathcal{L}_{\text{encdec}} = \sum_{k=1}^m \left\| x^{(k)} - \psi_{w_{\text{dec}}}(\phi_{w_{\text{enc}}}(x^{(k)})) \right\|^2. \quad (9)$$

ii) Quadratic dynamics for  $z$  given  $\dot{x}$ :

$$\mathcal{L}_{\dot{z}\dot{x}} = \sum_{k=1}^m \left\| \dot{z}^{(k)} - A(z^{(k)} \otimes z^{(k)}) - Bz^{(k)} - C \right\|^2, \quad (10)$$

where  $z^{(k)} = \phi_{w_{\text{enc}}}(x^{(k)})$ ,  $\dot{z}^{(k)} = J_{\phi_{w_{\text{enc}}}}(x^{(k)}) \dot{x}^{(k)}$ , and  $J_{\phi_{w_{\text{enc}}}}(x^{(k)})$  is the Jacobian matrix of the encoder map  $\phi_{w_{\text{enc}}}$  at  $x^{(k)}$  evaluated via automatic differentiation.

iii) Recovery of  $\dot{x}$  from the quadratic expression of  $\dot{z}$ :

$$\mathcal{L}_{\dot{x}\dot{z}} = \sum_{k=1}^m \left\| \dot{x}^{(k)} - J_{\psi_{w_{\text{dec}}}}(z^{(k)})(A(z^{(k)} \otimes z^{(k)}) + Bz^{(k)} + C) \right\|^2. \quad (11)$$

Overall, the goal is to solve the optimization problem

$$A, B, C, w_{\text{enc}}, w_{\text{dec}} = \arg \min_{\hat{A}, \hat{B}, \hat{C}, \hat{w}_{\text{enc}}, \hat{w}_{\text{dec}}} L(\hat{A}, \hat{B}, \hat{C}, \hat{w}_{\text{enc}}, \hat{w}_{\text{dec}}),$$

where  $L = \lambda_1 \mathcal{L}_{\text{encdec}} + \lambda_2 \mathcal{L}_{\dot{x}\dot{z}} + \lambda_3 \mathcal{L}_{\dot{z}\dot{x}}$  and  $\lambda_i$ ,  $i \in \{1, 2, 3\}$  are non-negative hyperparameters that need to be tuned. The norm  $\|\cdot\|$  used in (9)–(11) is defined to be  $\|\cdot\| = \|\cdot\|_2 + \kappa \|\cdot\|_1$ , where  $\kappa$  is typically between 0 and 1. It is important to note that in the implementation of the method, the authors of [28] use iterative hard thresholding to promote sparsity in the learned matrices  $A$  and  $B$ . Therefore, the method requires tuning five hyperparameters (the  $\lambda_i$ ,  $\kappa$  and the hard thresholding level) that all have an effect on its performance. The structure and size of the encoder and decoder networks, and optimization-related hyperparameters such as the learning rate and the batch size also play a pivotal role on the performance of the method in practice.

### 3.7. Summary

The above analysis shows that QENDy and SINDy are closely related, the quadratic embedding just generates a higher-dimensional feature space by using not only the basis functions themselves but also products of basis functions. However, QENDy approximates  $\nabla \phi_\ell \cdot F$  for  $\ell = 1, \dots, N$ , from which we then extract  $F$  using (3), whereas SINDy approximates  $F_\ell$  for  $\ell = 1, \dots, n$ . Furthermore, QENDy learns a quadratic system, while the SINDy model still requires evaluating the typically nonlinear basis functions. The deep learning approach identifies not only  $A$ ,  $B$ , and  $C$ , but also the nonlinear transformation itself, which makes it more flexible, but less interpretable. The learned models, however, do often not generalize to unseen data, i.e., they are suitable for interpolation but not necessarily extrapolation. QENDy, on the other hand, identifies a globally defined model whose accuracy depends strongly on the chosen dictionary.

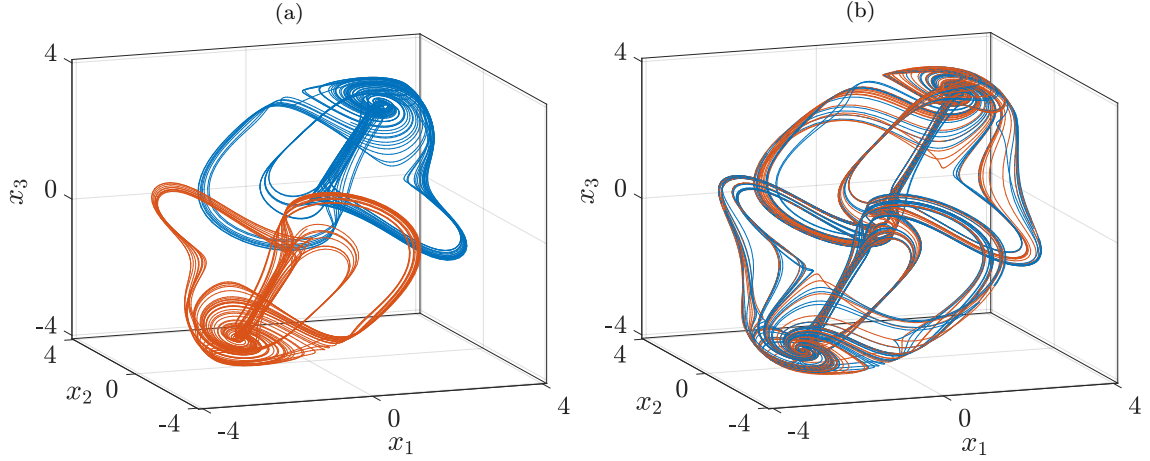


**Figure 2:** Simulation of the modified Thomas system with (a)  $\alpha = 0.2$  and  $\beta = 0$  and (b)  $\alpha = 0.25$  and  $\beta = 0.15$  using two randomly generated initial conditions.

## 4. Numerical results

In this section, we will present numerical results for various benchmark problems.

### 4.1. Modified Thomas attractor

Consider the system

$$\begin{bmatrix} \dot{x}_1 \\ \dot{x}_2 \\ \dot{x}_3 \end{bmatrix} = \begin{bmatrix} \sin(x_2) - \alpha x_1 - \beta x_2 \cos(x_1) \\ \sin(x_3) - \alpha x_2 - \beta x_3 \cos(x_2) \\ \sin(x_1) - \alpha x_3 - \beta x_1 \cos(x_3) \end{bmatrix},$$

where  $\alpha$  and  $\beta$  are parameters. If  $\beta = 0$ , we obtain the original Thomas attractor [41] as a special case. We consider two different test cases: (a)  $\alpha = 0.2$  and  $\beta = 0$  and (b)  $\alpha = 0.25$  and  $\beta = 0.15$ . Trajectories for both parameter settings are shown in Figure 2. We then define

$$z = \begin{bmatrix} x_1 \\ x_2 \\ x_3 \\ \sin(x_1) \\ \sin(x_2) \\ \sin(x_3) \\ \cos(x_1) \\ \cos(x_2) \\ \cos(x_3) \end{bmatrix} \implies \dot{z} = \begin{bmatrix} z_5 - \alpha z_1 - \beta z_2 z_7 \\ z_6 - \alpha z_2 - \beta z_3 z_8 \\ z_4 - \alpha z_3 - \beta z_1 z_9 \\ z_5 z_7 - \alpha z_1 z_7 - \beta z_2 z_7^2 \\ z_6 z_8 - \alpha z_2 z_8 - \beta z_3 z_8^2 \\ z_4 z_9 - \alpha z_3 z_9 - \beta z_1 z_9^2 \\ -z_4 z_5 + \alpha z_1 z_4 + \beta z_2 z_4 z_7 \\ -z_5 z_6 + \alpha z_2 z_5 + \beta z_3 z_5 z_8 \\ -z_4 z_6 + \alpha z_3 z_6 + \beta z_1 z_6 z_9 \end{bmatrix}. \quad (12)$$

That is, if  $\beta = 0$ , the resulting system is quadratic in the embedding space. If, on the other hand,  $\beta \neq 0$ , the first three terms are still quadratic, but the remaining equations are of order three and would require introducing additional basis functions, see Appendix B.

**First test case.** In order to learn the quadratic embedding of the dynamics, we generate one long trajectory consisting of 1000 training data points by simulating the Thomas system with initial condition  $x_0 = [1, -1, 0]^\top$  for  $t \in [0, 100]$ . We then compute the corresponding time derivatives and apply QENDy. The resulting matrices  $A$  and  $B$  are sparse and the vector  $C$  is zero as shown in Figure 3(a). We simulate the quadratic model identified by QENDy using the initial condition

$x_0 = [0, 1, 1]^\top$  and compare the trajectory with the corresponding SINDy model and the true dynamics. The numerical results are shown in Figure 3(c). QENDy successfully learns the correct quadratic embedding and the identified model is a very good approximation of the original dynamics. However, since the system is chaotic, even small numerical errors will eventually lead to large deviations. SINDy also works in this case as the right-hand side can be written as a linear combination of the basis functions, provided that  $\beta = 0$ .

**Second test case.** Although the right-hand side of the modified Thomas system can be written in terms of the quadratically augmented basis, the chosen basis functions are not sufficient for recasting the system as a quadratic model as shown in (12). Applying again QENDy, the matrices  $A$  and  $B$  and the vector  $C$  are not sparse anymore, see Figure 3(b). Also SINDy with the chosen dictionary fails to correctly identify the system. Both methods nevertheless allow us to learn approximations of the true dynamics as illustrated in Figure 3(d). We could in this case define

$$\dot{x} = GA(\phi(x) \otimes \phi(x)) + GB\phi(x) + GC,$$

which would be the correct model. This can be viewed as a combination of QENDy and SINDy, where we use the quadratically augmented basis to learn the right-hand side instead of a quadratic embedding. In order to obtain a valid quadratic embedding, we would have to choose a larger dictionary.

**Remark 4.1.** Additionally, we also applied the deep learning approach to both test cases. For the encoder mapping, we use a neural network with three fully-connected hidden layers of 64 units each and ELU activation functions. We set the embedding dimension to four and choose  $\lambda_1 = 0.05$ ,  $\lambda_2 = 0.1$ ,  $\lambda_3 = 1$ , and  $\kappa = 0$ . These settings were chosen after manual hyperparameter tuning. Following the original implementation published along with [28], we use a linear mapping for the decoder. Despite extensive hyperparameter tuning, the deep learning approach did not yield a good approximation for either test case and we therefore do not show the results.

## 4.2. Kármán vortex street

We now consider fluid flow past a cylinder in two dimensions at Reynolds number 100. This system is governed by partial differential equations. We discretize the domain using a regular  $520 \times 180$  grid and compute the vorticities in the grid points for  $t = 0, \dots, 499$  as shown in Figure 4(a)–(c). We then store the numerically computed vorticities in a three-dimensional array  $V \in \mathbb{R}^{180 \times 520 \times 500}$  and apply *Principal Component Analysis* (PCA). There are three dominant principal components, shown in Figure 4(d)–(f), followed by a spectral gap. That is, despite the high-dimensional state space caused by the grid discretization, the dynamics are approximately three-dimensional. By projecting the time-series data onto the dominant principal components, we obtain a three-dimensional dynamical system. It was shown in the Supporting Information supplementing [29] that SINDy successfully identifies an ordinary differential equation that approximates the dynamics in the three-dimensional principal component space. Our goal is to compute a quadratic model using QENDy. We choose  $z = x$ , i.e., the embedding space is the original projected principal component space, and estimate the required time derivatives with the aid of finite difference approximations (using a forward difference for the first data point, a backward difference for the last data point, and central differences in between). We apply QENDy to the first 400 data points and then simulate the identified quadratic model for  $t \in [0, 500]$ . Furthermore, we also apply the deep learning approach proposed in [28] using a neural network with two fully connected layers of twelve units each for the encoder map and a linear mapping for the decoder. Based on extensive manual hyperparameter tuning, we set the embedding dimension to four, the loss weights to  $\lambda_1 = 1$ ,  $\lambda_2 = 40$ , and  $\lambda_3 = 80$ ,

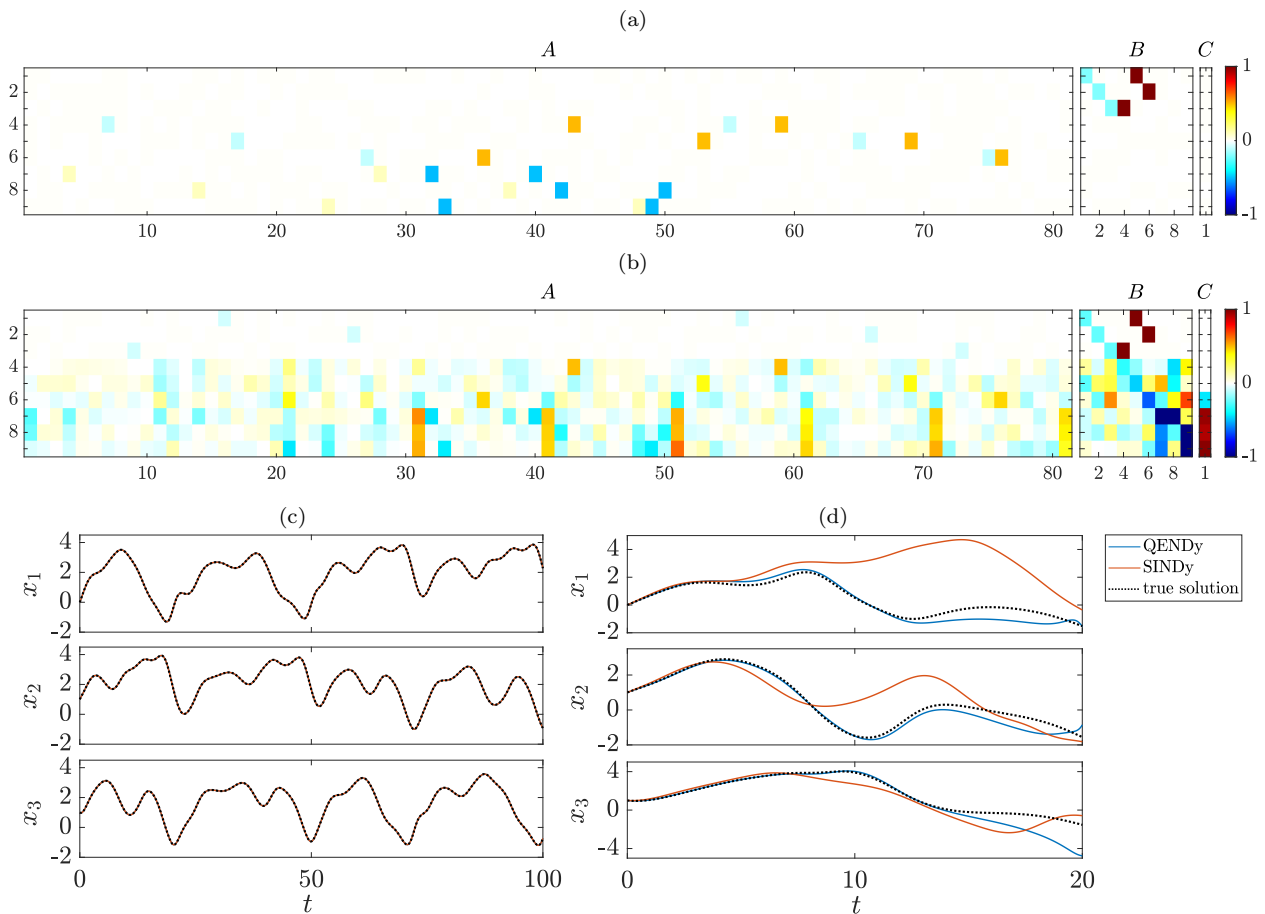


**Figure 3:** (a) Identified system for  $\alpha = 0.2$  and  $\beta = 0$ . (b) Identified system for  $\alpha = 0.25$  and  $\beta = 0.15$ . Only the first three rows are sparse since the functions  $\dot{z}_4, \dots, \dot{z}_9$  are not contained in the space spanned by the augmented basis. (c) Comparison of the QENDy model, the SINDy model, and the true dynamics for the first test case. Both methods correctly identify the governing equations and the numerical solutions coincide. (d) Comparison of the QENDy model, the SINDy model, and the true dynamics for the second test case. The learned models only allow us to make short-term predictions in this case. The QENDy approximation is slightly more accurate, but both models deviate or become unstable for larger  $t$ .

and  $\kappa = 0$ . The results for both methods are shown in Figure 4(g) and Figure 4(h). The learned quadratic models are good approximations of the projected dynamics and correctly predict the periodic behavior, even though we do not know the true underlying system. QENDy—using only linear basis functions—is in this case slightly more accurate than the neural network approximation.

## 5. Conclusion

We have derived a method called QENDy that allows us to learn quadratic embeddings of nonlinear dynamical systems from simulation or measurement data and can be viewed as a combination of SINDy [29] and the deep learning method proposed in [28]. Given a fixed set of basis functions, the computation of the optimal embedding just requires solving systems of linear equations in the least squares sense. We have shown that in the infinite data limit we obtain the best approximation of the dynamics with respect to a weighted inner product that depends on the sampling of the training data points. While SINDy directly approximates the governing equations using the selected basis



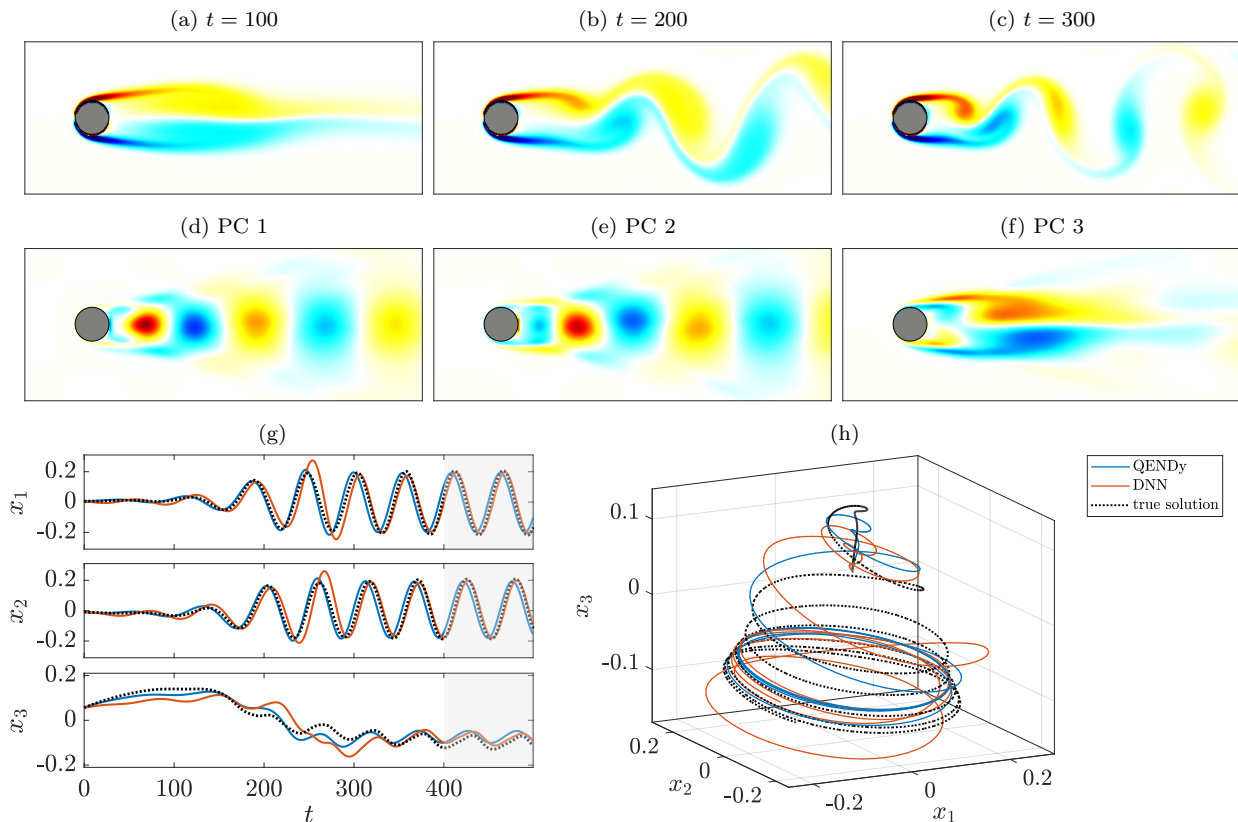


**Figure 4:** (a)–(c) Vorticities of the simulated Kármán vortex street at different times  $t$ . After the transient phase, the system exhibits the well-known periodic vortex shedding. (d)–(f) The first three principal components. (g) Comparison of the QENDy model, the deep learning approach, and the true dynamics. The area shaded in gray is the extrapolation domain, i.e., these points are not contained in the training data set. (h) Three-dimensional plot of the results. The trajectories converge to the limit cycle representing the periodic vortex shedding.

functions, QENDy uses a quadratically augmented basis. Our results also explain the purported superior performance of deep learning based quadratic embedding techniques compared to linear methods, which seems to be mostly due to the fact that these methods implicitly generate a larger and thus more expressive feature space. In general, QENDy will not result in a quadratic embedding that perfectly reproduces the dynamics—unless we have prior information about the terms appearing in the governing equations and choose a suitable dictionary—, but nevertheless computes the best approximation, which allows for short-term forecasting. The sparsity of the matrices  $A$  and  $B$  is typically a good indicator for the accuracy of the learned model. If the matrices are not sparse, this implies that almost all basis functions are required to approximate missing terms.

Although the numerical results show that QENDy works well for simple benchmark problems, many open questions remain: High-dimensional systems will in general require a large set of basis functions, which significantly increases the number of parameters we have to estimate. A possible extension would be to develop a kernel-based variant of QENDy, which implicitly works in a potentially infinite-dimensional feature space rather than an explicitly constructed space spanned by a set of basis functions. This would allow us to circumvent the curse of dimensionality. The drawback is that then the dimensions of the matrices depend on the number of training data points. Alternatively, low-rank tensor approximations as proposed in [42] could be used to compress the data matrices. Furthermore, instead of using Tikhonov regularization, it would also be possible

to use iterative hard thresholding or  $\ell_1$  regression techniques to promote sparsity. Another open question is whether it is possible to incorporate physical constraints such as energy conservation laws or symplecticity and also to guarantee the stability of the learned model. A second-order accurate integrator tailored to quadratic systems has been proposed in [43], the question is whether the method is more robust than conventional integrators or preserves certain properties of the underlying system.

## Acknowledgments

We would like to thank Feliks Nüske and Peter Benner for interesting discussions about the quadratic embedding framework.

## References

- [1] B. Koopman. Hamiltonian systems and transformations in Hilbert space. *Proceedings of the National Academy of Sciences*, 17(5):315, 1931. doi:10.1073/pnas.17.5.315.
- [2] A. Lasota and M. C. Mackey. *Chaos, fractals, and noise: Stochastic aspects of dynamics*, volume 97 of *Applied Mathematical Sciences*. Springer, New York, 2nd edition, 1994.
- [3] I. Mezić. Spectral properties of dynamical systems, model reduction and decompositions. *Nonlinear Dynamics*, 41(1):309–325, 2005. doi:10.1007/s11071-005-2824-x.
- [4] M. Budišić, R. Mohr, and I. Mezić. Applied Koopmanism. *Chaos: An Interdisciplinary Journal of Nonlinear Science*, 22(4), 2012. doi:10.1063/1.4772195.
- [5] M. O. Williams, I. G. Kevrekidis, and C. W. Rowley. A data-driven approximation of the Koopman operator: Extending dynamic mode decomposition. *Journal of Nonlinear Science*, 25(6):1307–1346, 2015. doi:10.1007/s00332-015-9258-5.
- [6] S. Klus, P. Koltai, and C. Schütte. On the numerical approximation of the Perron–Frobenius and Koopman operator. *Journal of Computational Dynamics*, 3(1):51–79, 2016. doi:10.3934/jcd.2016003.
- [7] C. Schütte and M. Sarich. *Metastability and Markov State Models in Molecular Dynamics: Modeling, Analysis, Algorithmic Approaches*. Number 24 in Courant Lecture Notes. American Mathematical Society, 2013.
- [8] A. Mauroy and I. Mezić. Global stability analysis using the eigenfunctions of the Koopman operator. *IEEE Transactions on Automatic Control*, 61(11):3356–3369, 2016. doi:10.1109/TAC.2016.2518918.
- [9] A. Mauroy and J. Goncalves. Linear identification of nonlinear systems: A lifting technique based on the Koopman operator. In *2016 IEEE 55th Conference on Decision and Control (CDC)*, pages 6500–6505, 2016. doi:10.1109/CDC.2016.7799269.
- [10] M. Korda and I. Mezić. Linear predictors for nonlinear dynamical systems: Koopman operator meets model predictive control. *Automatica*, 93:149–160, 2018. doi:10.1016/j.automatica.2018.03.046.
- [11] S. Peitz and S. Klus. Koopman operator-based model reduction for switched-system control of PDEs. *Automatica*, 106:184–191, 2019. doi:10.1016/j.automatica.2019.05.016.

- [12] S. Klus, F. Nüske, S. Peitz, J.-H. Niemann, C. Clementi, and C. Schütte. Data-driven approximation of the Koopman generator: Model reduction, system identification, and control. *Physica D: Nonlinear Phenomena*, 406:132416, 2020. doi:10.1016/j.physd.2020.132416.
- [13] P. Bevanda, S. Sosnowski, and S. Hirche. Koopman operator dynamical models: Learning, analysis and control. *Annual Reviews in Control*, 52:197–212, 2021. doi:doi.org/10.1016/j.arcontrol.2021.09.002.
- [14] S. Klus and N. Djurdjevic Conrad. Dynamical systems and complex networks: A Koopman operator perspective. *Journal of Physics: Complexity*, 2024. doi:10.1088/2632-072X/ad9e60.
- [15] T. Carleman. Application de la théorie des équations intégrales linéaires aux systèmes d'équations différentielles non linéaires. *Acta Mathematica*, 59:63–87, 1932. doi:10.1007/BF02546499.
- [16] K. Kowalski and W.-H. Steeb. *Nonlinear dynamical systems and Carleman linearization*. World Scientific, 1991.
- [17] D. Shi and X. Yang. Koopman spectral linearization vs. Carleman linearization: A computational comparison study. *Mathematics*, 12(14), 2024. doi:10.3390/math12142156.
- [18] E. H. Kerner. Universal formats for nonlinear ordinary differential systems. *Journal of Mathematical Physics*, 22(7):1366–1371, 1981.
- [19] C. Gu. QLMOR: A projection-based nonlinear model order reduction approach using quadratic-linear representation of nonlinear systems. *IEEE Transactions on Computer-Aided Design of Integrated Circuits and Systems*, 30(9):1307–1320, 2011.
- [20] G. G. Appelroth. La forme fondamentale du système d'équations différentielles algébriques. *Matematicheskii Sbornik*, 23(1):12–23, 1902.
- [21] M. A. Savageau and E. O. Voit. Recasting nonlinear differential equations as S-systems: a canonical nonlinear form. *Mathematical Biosciences*, 87(1):83–115, 1987.
- [22] A. Papachristodoulou and S. Prajna. Analysis of non-polynomial systems using the sum of squares decomposition. In *Positive polynomials in control*, pages 23–43. Springer Berlin Heidelberg, 2005.
- [23] J. Liu, N. Zhan, H. Zhao, and L. Zou. Abstraction of elementary hybrid systems by variable transformation. In *International Symposium on Formal Methods*, pages 360–377, Cham, 2015. Springer International Publishing.
- [24] F. Carravetta. Global exact quadratization of continuous-time nonlinear control systems. *SIAM Journal on Control and Optimization*, 53(1):235–261, 2015. doi:10.1137/130915418.
- [25] B. Kramer and K. E. Willcox. Nonlinear model order reduction via lifting transformations and proper orthogonal decomposition. *AIAA Journal*, 57(6):2297–2307, 2019.
- [26] Y. Cai and G. Pogudin. Dissipative quadratizations of polynomial ODE systems. In *International Conference on Tools and Algorithms for the Construction and Analysis of Systems*, pages 323–342, 2024.
- [27] A. Bychkov, O. Issan, G. Pogudin, and B. Kramer. Exact and optimal quadratization of nonlinear finite-dimensional nonautonomous dynamical systems. *SIAM Journal on Applied Dynamical Systems*, 23(1):982–1016, 2024. doi:10.1137/23M1561129.

- [28] P. Goyal and P. Benner. Generalized quadratic embeddings for nonlinear dynamics using deep learning. *Physica D: Nonlinear Phenomena*, 463:134158, 2024. doi:10.1016/j.physd.2024.134158.
- [29] S. L. Brunton, J. L. Proctor, and J. N. Kutz. Discovering governing equations from data by sparse identification of nonlinear dynamical systems. *Proceedings of the National Academy of Sciences*, 113(15):3932–3937, 2016.
- [30] B. Peherstorfer and K. Willcox. Data-driven operator inference for nonintrusive projection-based model reduction. *Computer Methods in Applied Mechanics and Engineering*, 306:196–215, 2016. doi:10.1016/j.cma.2016.03.025.
- [31] F. Noé and F. Nüske. A variational approach to modeling slow processes in stochastic dynamical systems. *Multiscale Modeling & Simulation*, 11(2):635–655, 2013.
- [32] M. C. Bañuls, R. Orús, J. I. Latorre, A. Pérez, and P. Ruiz-Femenia. Simulation of many-qubit quantum computation with matrix product states. *Physical Review A*, 73:022344, 2006. doi:10.1103/PhysRevA.73.022344.
- [33] I. Oseledets. Tensor-train decomposition. *SIAM Journal on Scientific Computing*, 33:2295–2317, 2011. doi:10.1137/090752286.
- [34] K. B. Petersen and M. S. Pedersen. *The Matrix Cookbook*, 2012.
- [35] B. Kramer. Stability domains for quadratic-bilinear reduced-order models. *SIAM Journal on Applied Dynamical Systems*, 20(2):981–996, 2021. doi:10.1137/20M1364849.
- [36] N. Sawant, B. Kramer, and B. Peherstorfer. Physics-informed regularization and structure preservation for learning stable reduced models from data with operator inference. *Computer Methods in Applied Mechanics and Engineering*, 404:115836, 2023. doi:10.1016/j.cma.2022.115836.
- [37] G-R. Duan and R.J. Patton. A note on Hurwitz stability of matrices. *Automatica*, 34(4):509–511, 1998. doi:10.1016/S0005-1098(97)00217-3.
- [38] P. Goyal, I. Pontes Duff, and P. Benner. Guaranteed stable quadratic models and their applications in sindy and operator inference, 2023. URL: <https://arxiv.org/abs/2308.13819>, arXiv:2308.13819.
- [39] L. Boninsegna, F. Nüske, and C. Clementi. Sparse learning of stochastic dynamical equations. *The Journal of Chemical Physics*, 148(24):241723, 2018. doi:10.1063/1.5018409.
- [40] S. H. Rudy, S. L. Brunton, J. L. Proctor, and J. N. Kutz. Data-driven discovery of partial differential equations. *Science Advances*, 3(4):e1602614, 2017. doi:10.1126/sciadv.1602614.
- [41] R. Thomas. Deterministic chaos seen in terms of feedback circuits: Analysis, synthesis, “labyrinth chaos”. *International Journal of Bifurcation and Chaos*, 9(10):1889–1905, 1999. doi:10.1142/S0218127499001383.
- [42] P. Gelß, S. Klus, J. Eisert, and C. Schütte. Multidimensional approximation of nonlinear dynamical systems. *Journal of Computational and Nonlinear Dynamics*, 14:061006, 2019. doi:10.1115/1.4043148.
- [43] W. Kahan and R.-C. Li. Unconventional schemes for a class of ordinary differential equations—with applications to the Korteweg–de Vries equation. *Journal of Computational Physics*, 134(2):316–331, 1997.

- [44] F. Deutsch. *Best approximation in inner product spaces*. CMS Books in Mathematics. Springer, 2001.
- [45] H. R. Schwarz and N. Köckler. *Numerische Mathematik*. Vieweg+Teubner Verlag, Wiesbaden, 8th edition, 2011. doi:10.1007/978-3-8348-8166-3.
- [46] G. H. Golub and C. F. Van Loan. *Matrix Computations*. Johns Hopkins University Press, 4th edition, 2013.

## A. Best approximation

Let  $H$  be a real Hilbert space with inner product  $\langle \cdot, \cdot \rangle$  and induced norm  $\|\cdot\| = \langle \cdot, \cdot \rangle^{\frac{1}{2}}$ . Furthermore, let  $\{\phi_1, \dots, \phi_n\} \subset H$  be a set of basis vectors spanning the linear subspace  $V = \text{span}\{\phi_1, \dots, \phi_n\}$ . Any element  $g \in V$  can be written as

$$g = \sum_{i=1}^n \alpha_i \phi_i = \alpha^\top \phi,$$

where  $\alpha = [\alpha_1, \dots, \alpha_n]^\top \in \mathbb{R}^n$ . Note that this representation is unique only if the basis vectors are linearly independent. Given an arbitrary vector  $f \in H$ , we want to find  $g \in V$  such that the error

$$E(\alpha) := \|f - g\|^2 = \langle f, f \rangle - 2 \sum_{i=1}^n \alpha_i \langle \phi_i, f \rangle + \sum_{i=1}^n \sum_{j=1}^n \alpha_i \alpha_j \langle \phi_i, \phi_j \rangle \quad (13)$$

is minimized, i.e.,  $g$  is the best approximation of  $f$  contained in the subspace  $V$ . Defining  $A \in \mathbb{R}^{n \times n}$  and  $b \in \mathbb{R}^n$ , with  $a_{ij} = \langle \phi_i, \phi_j \rangle$  and  $b_i = \langle \phi_i, f \rangle$ , we have

$$E(\alpha) = \langle f, f \rangle - 2b^\top \alpha + \alpha^\top A \alpha \implies \nabla E(\alpha) = -2b + 2A\alpha.$$

In order to find optimal solutions, we thus have to solve the system of linear equations

$$A\alpha = b. \quad (14)$$

**Theorem A.1.** *Let the basis vectors  $\{\phi_1, \dots, \phi_n\}$  be linearly independent. Then the matrix  $A$  is symmetric and positive definite and the unique minimizer of (13) is given by (14).*

*Proof.* See, e.g., [44, 45]. □

The matrix  $A$  is non-singular if and only if the basis vectors are linearly independent. In our setting, however, this is in general not the case. Assume that

$$V = \text{span}\{\phi_1, \dots, \phi_n\} = \text{span}\{\phi_1, \dots, \phi_r\},$$

with  $r < n$ , i.e., the basis vectors span only an  $r$ -dimensional vector space. Thus,

$$\phi_k = \sum_{i=1}^r \beta_{ki} \phi_i, \quad \text{for } k = r+1, \dots, n.$$

Consider now the  $k$ th rows of  $A$  and  $b$ , with  $k > r$ , then

$$A_{kj} = \langle \phi_k, \phi_j \rangle = \sum_{i=1}^r \beta_{ki} \langle \phi_i, \phi_j \rangle = \sum_{i=1}^r \beta_{ki} a_{ij},$$

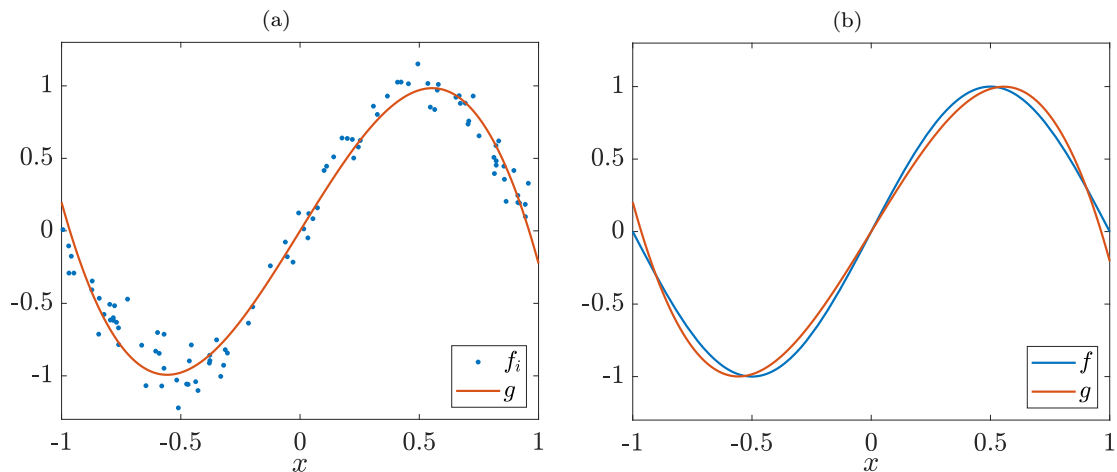


**Figure 5:** (a) Approximation of the data points  $(x_i, f_i)$  by a polynomial of degree 3. (b) Approximation of  $\sin(\pi x)$  by a polynomial of degree 3.

$$b_k = \langle \phi_k, f \rangle = \sum_{i=1}^r \beta_{ki} \langle \phi_i, f \rangle = \sum_{i=1}^r \beta_{ki} b_i.$$

The last  $n - r$  rows of  $A$  and  $b$  are hence the same linear combinations of the first  $r$  rows of  $A$  and  $b$ . It follows that the rank of the augmented matrix  $[A \mid b]$  is  $r$ , which is also the rank of  $A$ . That is, the system (14) is consistent and there is an infinite number of solutions. Let  $\tilde{A}$  be the submatrix comprising the first  $r$  rows and columns of  $A$ ,  $\tilde{b}$  the first  $r$  rows of  $b$ , and  $\tilde{\alpha}$  the unique solution of  $\tilde{A}\tilde{\alpha} = \tilde{b}$ , then the vector

$$\alpha_p = \begin{bmatrix} \tilde{\alpha} \\ 0 \end{bmatrix} \in \mathbb{R}^n$$

is a particular solution of (14). Adding any vector  $u$  contained in the null space of  $A$  will also result in a valid solution. Defining  $\alpha = A^+b$  picks the solution with the smallest 2-norm, see [46].

**Example A.2.** We have to distinguish between discrete and continuous best approximation:

i) Assume we have data  $\{(x_i, f_i)\}_{i=1}^m$ , with  $x_i, f_i \in \mathbb{R}$  and we want to find a function

$$g(x) = \sum_{i=1}^n \alpha_i \hat{\phi}_i(x)$$

that approximates the data. We define the vectors  $\phi_i = [\hat{\phi}_i(x_1), \dots, \hat{\phi}_i(x_m)]^\top \in \mathbb{R}^m$  and  $f = [f_1, \dots, f_m]^\top \in \mathbb{R}^m$ . Solving the resulting system of linear equations (14), we obtain the coefficients  $\alpha$ . The Hilbert space is  $H = \mathbb{R}^m$ , with inner product  $\langle f, g \rangle = \sum_{i=1}^m f_i g_i \mu_i$ , where  $\mu_i > 0$  is the weight for the data point  $x_i$ .

ii) Assume we want to approximate the function  $f(x)$  in the interval  $[a, b]$  by a function of the form

$$g(x) = \sum_{i=1}^n \alpha_i \phi_i(x).$$

We choose  $H = L_\mu^2([a, b])$ , i.e., the space of square-integrable functions with respect to a measure  $\mu$ , with inner product  $\langle f, g \rangle_\mu = \int_a^b f(x)g(x)d\mu(x)$ , and again compute  $\alpha$  by solving (14). The difference between discrete and continuous best approximation problems is also illustrated in Figure 5.  $\triangle$

## B. Quadratic embedding of the modified Thomas attractor

As shown in Section 4, the nine-dimensional feature space defined in (12) is not sufficient for the modified Thomas attractor. In order to find a quadratic embedding, we augment the feature space as follows:

$$z = \begin{bmatrix} x_1 \\ x_2 \\ x_3 \\ \sin(x_1) \\ \sin(x_2) \\ \sin(x_3) \\ \cos(x_1) \\ \cos(x_2) \\ \cos(x_3) \\ x_2 \sin(x_1) \\ x_3 \sin(x_2) \\ x_1 \sin(x_3) \\ x_2 \cos(x_1) \\ x_3 \cos(x_2) \\ x_1 \cos(x_3) \end{bmatrix} \implies \dot{z} = \begin{bmatrix} z_5 - \alpha z_1 - \beta z_{13} \\ z_6 - \alpha z_2 - \beta z_{14} \\ z_4 - \alpha z_3 - \beta z_{15} \\ z_5 z_7 - \alpha z_1 z_7 - \beta z_7 z_{13} \\ z_6 z_8 - \alpha z_2 z_8 - \beta z_8 z_{14} \\ z_4 z_9 - \alpha z_3 z_9 - \beta z_9 z_{15} \\ -z_4 z_5 + \alpha z_1 z_4 + \beta z_4 z_{13} \\ -z_5 z_6 + \alpha z_2 z_5 + \beta z_5 z_{14} \\ -z_4 z_6 + \alpha z_3 z_6 + \beta z_1 z_{15} \\ (z_4 z_6 + z_5 z_{13}) - \alpha(z_1 z_{13} + z_2 z_4) - \beta(z_4 z_{14} + z_{13}^2) \\ (z_4 z_5 + z_6 z_{14}) - \alpha(z_2 z_{14} + z_3 z_5) - \beta(z_5 z_{15} + z_{14}^2) \\ (z_4 z_{15} + z_5 z_6) - \alpha(z_1 z_6 + z_3 z_{15}) - \beta(z_6 z_{13} + z_{15}^2) \\ (-z_5 z_{10} + z_6 z_7) - \alpha(-z_1 z_{10} + \alpha z_2 z_7) - \beta(z_7 z_{14} - z_{10} z_{13}) \\ (z_4 z_8 - z_6 z_{11}) - \alpha(-z_2 z_{11} + z_3 z_8) - \beta(-z_{11} z_{14} + z_8 z_{15}) \\ (-z_4 z_{12} + z_5 z_9) - \alpha(z_1 z_9 - \alpha z_3 z_{12}) - \beta(z_9 z_{13} - \beta z_{12} z_{15}) \end{bmatrix}.$$

The representation, however, is not unique. Using this set of basis functions, QENDy successfully learns a valid quadratic model and the matrices  $A$  and  $B$  are again sparse.